Ai et al. AAPS Open (2024) 10:9
https://doi.org/10.1186/s41120-024-00099-8

AAPS Open

RESEARCH Open Access

# Characterization, stability, and skin application of astaxanthin particulates

Miyu Ai[1], Risa Kanai[2], Hiroaki Todo[2], Junki Tomita[3], Takashi Tanikawa[1] and Yutaka Inoue[1*]

## Abstract

**Purpose** Astaxanthin (AX), commonly used for dermal applications, exhibits anti-inflammatory and antioxidant activities; however, it has poor water solubility. In this study, we investigated the physicochemical properties of AX-containing particulates formulated using the amphiphilic graft copolymer Soluplus (polyvinyl caprolactam-polyvinyl acetate-polyethylene glycol graft copolymer: Sol) and polyethylene glycol-2000 (PEG 2000); in addition, the stability and skin applications of AX particulates were investigated.

**Methods** AX, Sol, and PEG were mixed by weight to prepare AX particles using the hydration method. The prepared particles were subjected to stability evaluations including particle size distribution, zeta potential estimation, and fluorescence spectroscopy as well as physical evaluations including $^{1}$H-$^{1}$H NOESY NMR spectral measurement, powder X-ray diffraction, and differential scanning calorimetry. Functional evaluations included singlet oxygen scavenging, skin permeation test, and fluorescence microscopy.

**Results** Relatively stable particles of Sol/AX and Sol/PEG 2000/AX, approximately 100 nm and 125 nm in size, respectively, were formed at a mixed weight ratio (9/1) of 0.1 M Ascorbic Acid solution (0.1 M ASC) and a mixed weight ratio (8/1/1) of 0.1 M ASC, respectively, at 25 °C after storage for 14 days under light-shielded condition. Stability evaluations revealed a decrease in fluorescence intensity and color fading for Sol/AX = 9/1 and Sol/PEG 2000/AX = 8/1/1 (dispersion medium: distilled water); however, no change in fluorescence intensity of AX was observed immediately after preparation in Sol/AX = 9/1 and Sol/PEG 2000/AX = 8/1/1 (dispersion medium: 0.1 M ASC). The fluorescence intensity of AX did not fluctuate significantly immediately after adjustment, and the particles remained stable, showing a bright orange color with time. NMR spectra of Sol/AX = 9/1 and Sol/PEG 2000/AX (dispersion medium: 0.1 M ASC) showed the interactions between the $CH_3$ group e from Sol (1.8 ~ 2.0 ppm) and the CH groups H-15,11 from AX (6.7 ~ 6.8 ppm), 8′,12′ (6.4 ~ 6.5 ppm), H-10,14 (6.4 ~ 6.5 ppm), and 7,7′ (6.2 ~ 6.3 ppm), indicating the disappearance of cross peaks. Furthermore, new cross peaks were identified for the $CH_3$ group e of Sol (1.8 ~ 2.0 ppm), the 7-membered ring z of Sol (1.5 ~ 1.8 ppm), the 5-membered ring S of ASC (3.5 ~ 3.6 ppm), the CH group T (3.8 ~ 3.9 ppm), and the CH group U (4.7 ppm). Fluorescence microscopy observations of microparticles formulated with Sol/PEG 2000/AX showed a slight improvement in skin penetration.

**Conclusion** New AX particulates were formed using Sol/PEG 2000/AX = 8/1/1, suggesting that Sol/PEG 2000/AX maintained the stability and improved the skin penetration of AX.

**Keywords** Astaxanthin, Particulates, Stability, NMR spectrum, Skin penetration

*Correspondence:
Yutaka Inoue
yinoue@josai.ac.jp
Full list of author information is available at the end of the article

## Introduction

Astaxanthin (AX) is a red dye derived from marine organisms, including crustaceans and algae; it possesses high antioxidant activity (Shimidzu et al. 1996; Martinez-Alvarez et al. 2020; Zarneshan et al. 2020). The antioxidant capacity of AX against singlet oxygen, which is highly toxic, is reported to be approximately 40 times that of β-carotene and 550 times that of vitamin E (Shimidzu et al. 1996). AX has been reported to have significant physiological effects, such as reducing eye strain (Sekikawa et al. 2023), moisturizing and maintaining skin elasticity (Tsukahara et al. 2016), anti-inflammatory (Kohandel et al. 2015; Chang and Xiong 2020), and anti-diabetic (Landon et al. 2020). It is commonly used in nutraceutical (Davinelli et al. 2018), cosmetic (Alves et al. 2020), and pharmaceutical industries (Patil et al. 2022) owing to its diverse physiological actions (Zheng et al. 2013). However, its complicated structure consisting of polyene chains makes AX susceptible to oxygen, temperature, light, and pH, and exposure to these factors leads to the loss of functional properties and coloration (Wang et al. 2008; Ren et al. 2021). AX also has physicochemical property challenges, such as poor water solubility and low bioavailability (Odeberg et al. 2003). Therefore, it is necessary to make novel formulations of AX to further explore its applications. To date, various methods, such as β-cyclodextrin complexes (Kim et al. 2010), liposomes (Gulzar and Benjakul 2020), and nanoencapsulation (Zhu et al. 2015), have been investigated.

In recent years, various nano-based drug delivery systems (nanoDDS), such as liposomes, solid lipid nanoparticles, emulsions, and micelles, have been developed in the pharmaceutical, cosmetic, and food industries, depending on the delivery route (Onoue et al. 2014). NanoDDS improve the stability, efficacy, physicochemical properties, and pharmacokinetics of drugs. They alter the route of administration, reduce the frequency of administration, and suppress side effects by targeting specific tissues (Mishra et al. 2009; Onoue et al. 2014; Oku 2017). The physicochemical properties and applications of nanocarriers can be changed by modifying their surface properties in terms of composition, shape, surface charge, functional groups, and PEGylation (Zhang et al. 2014). As a typical example, the antitumor drug doxorubicin has been encapsulated in liposomes, and PEGylation has been reported to prolong the circulation time of the drug (Barenholz 2012; Suk et al. 2016; Oku 2017). In addition, clinical trial of NK105, a formulation of paclitaxel encapsulated in polymeric micelles, is currently underway (Kosaka et al. 2022).

Soluplus® (Sol: polyvinyl caprolactam-polyvinyl acetate-polyethylene glycol graft copolymer) is a graft copolymer with polyethylene glycol (PEG) backbone as the hydrophilic moiety and vinyl caprolactam/vinyl acetate side chains as the hydrophilic moiety (Pignatello et al. 2022). The amphiphilicity allows self-assembling of micelles in solutions with critical micelle concentrations exceeding 0.82 mg/mL (Tanida et al. 2016; Pignatello et al. 2022), which has been reported to improve the solubility of poorly water-soluble compounds such as itraconazole and enhance its bioavailability (Zhang et al. 2013). Furthermore, Soluplus acts as a stabilizer, allowing the formation of fine and stable particles (Yang et al. 2014). In our laboratory, we successfully prepared novel nanoparticles an amphiphilic copolymer of L-ascorbyl 2,6-dipalmitate (ASC-DP), an ascorbic acid derivative, using Soluplus. Nanoparticles encapsulating minoxidil were prepared to improve the drug delivery to the skin (Takayama et al. 2021). Moreover, a novel three-component nanoparticle preparation containing Soluplus® (Sol), ASC-DP, and nobiletin (NOB), a polymethoxyflavonoid, has been successfully developed, which is expected to inhibit melanin formation in the skin and exhibit antitumor activity (Inoue et al. 2022).

PEG is a polyether compound produced by the polymerization of ethylene oxide in the presence of water. This refers to oligomers and polymers with molecular weights of less than 20,000 g/mol (Jang et al. 2015). PEG has been used in various industries and pharmaceutical formulations owing to its diverse physicochemical properties and established safety, including high solubility in organic solvents and easily modifiable end functional groups (Özdemir and Güner 2007; Ibrahim et al. 2022). PEG can maintain particle stability by coating the surface of nanoparticles to form lipid nanoparticles, thereby preventing particle aggregation (Jung et al. 2016; Rahme and Dagher 2019). Inoue et al. reported successful preparation of nanoparticles to improve the skin penetration of nadifloxacin, a new quinolone antibacterial drug, using trisodium L-ascorbyl 2-phosphate 6-palmitate (APPS), an ascorbic acid derivative, and distearoyl phosphatidyl ethanolamine-PEG 2000 (DSPE-PEG 2000), a surfactant (Inoue et al. 2017).

The study was aimed to develop new microparticles of AX, an insoluble carotenoid, by mixing with Sol, an amphiphilic graft copolymer, and PEG, a surfactant, and to improve its functionality through the synergistic effects of Sol (solubilization by forming micelles) and PEG (stabilization by inhibiting aggregation). In addition, we aimed to expand the applications of AX through microparticle formulation in many fields, such as foods, pharmaceuticals, and skincare cosmetics. In this study, we prepared new particulates composed of Sol/PEG/AX using a hydration method and evaluated the stability and physicochemical properties of AX-containing

particulates. Moreover, skin permeation test and fluorescence microscopy observations were conducted to evaluate the skin application of AX.

## Materials and methods

### Materials

AX (20%) was obtained from Oryza Oil and Chemicals (Aichi, Japan, Lot: Y-115). Sol was provided by BASF Japan Ltd. (Tokyo, Japan, Lot: 84414368E0). PEG 2000 was purchased from Fujifilm Wako Pure Chemical Corporation (Osaka, Japan; Lot: WTN4311), and ASC-DP was purchased from Tokyo Kasei Kogyo Co., Ltd. (Tokyo, Japan, Lot: ISPKK-LH). NMR solvent (dimethyl sulfoxide-d6 [DMSO-d6]) was purchased from Cambridge Isotope Laboratories, Inc. (MA, USA). All other reagents were of special grade and purchased from Fujifilm Wako Pure Chemical Corporation.

### Methods

#### *Preparation of particulates*

The particulates were prepared using the hydration method (Inoue et al. 2017). In the hydration method, each lipid-soluble substance is dissolved in an organic solvent obtained by solvent distillation, and the prepared lipid film is hydrated with an aqueous solvent, such as distilled water (DW), to prepare a suspension. Sol, PEG, and AX were dissolved in chloroform each at a concentration of 1 mg/mL. Sol/PEG/AX and Sol/AX were sonicated for 1 min after mixing in a pear-shaped flask to a mixed weight ratio of 8/1/1 and 9/1, respectively. The critical micelle concentration of Sol was reported to be 0.82 mg/mL (Tanida et al. 2016). These samples were prepared at 40 °C by solvent distillation (Rotavapor R-215; Buchi, Switzerland). A thin film was then prepared by hydration of the prepared films with DW or 0.1 M ASC solution, followed by mixing in a vortex mixer for 1 min and sonication for 3 min.

#### *Particle size and zeta potential (ZP) measurements*

Mean particle size and polydispersity index measurements of the particles dispersed in solvent were performed using Zetasizer Nano ZS (Malvern Instruments, Malvern, UK). The ZP reflects the surface charge, which is thought to contribute to the stabilization of dispersed particles. One milliliter of each sample was added to a capillary cell, and measurements were performed under the following conditions: Set Zero 60 s (particle size), 120 s (ZP), 180 s measurement time, and 25 °C measurement temperature. Moreover, the suspension of the prepared particles in DW or 0.1 M ASC solution was kept under light-shielded condition at 25 °C for 14 days to evaluate the stability of the particles, and particle size distribution and ZP were measured on days 0, 1, 3, 5, 7, and 14.

#### *Colorimetric measurements*

Colorimetric measurements were performed using CR-400/410 (KONICA MINOLTA, Tokyo, Japan). Each sample was placed in a 1 cm × 1 cm on a white calibration plate ($n = 3$). To evaluate the stability of the microparticles, measurements were also performed after storage of the suspension obtained by dispersion in DW or 0.1 M ASC solution for 14 days (days 0, 1, 3, 5, 7, and 14) under light-shielded condition at 25 °C.

#### *Fluorescence spectroscopy*

The fluorescence spectra were measured using BioTek Synergy H1 (Agilent Technologies, CA, USA). Each sample (200 µL) was put onto a 96-well plate for fluorescence analysis, and measurements were performed under the following conditions: excitation wavelength (ex): 614 nm, fluorescence wavelength (em): 675 nm.

#### *Singlet oxygen scavenging activity*

Singlet oxygen scavenging capacity was measured using a near-infrared spectrofluorometer (FP-8700; Jasco) at an excitation wavelength (ex) of 520 nm and a fluorescence wavelength (em) of 1200–1350 nm to evaluate the antioxidant potential of AX in the prepared particulates. Phosphorescence derived from singlet oxygen using rose bengal (200 µM in 50% ethanol) as a photosensitizer was measured at approximately 1270 nm. L-histidine (25 mM) was used as positive control, and various samples were added to prepare a sample/rose bengal solution (1/1) mixture (final rose bengal concentration: 100 µM).

#### *Transmission electron microscopy (TEM)*

TEM was performed using HT7800 (Hitachi High-Tech, Ibaraki, Japan) at an acceleration voltage of 80 kV. Negative staining with 1% phosphotungstic acid was used.

#### *$^{1}$H-$^{1}$H Nuclear overhauser effect spectroscopy (NOESY) NMR experiment*

$^{1}$H-$^{1}$H NOESY NMR measurements were performed using AVANCE NEO 600 system (Bruker Japan, Kanagawa, Japan) with DMSO-d6 as solvent. The $^{1}$H chemical shift was based on the residual $D_2O$ signal (2.50 ppm). The resonance frequency was 600.1 MHz, pulse width was 8.00 µs, relaxation time was 0.800 s, integration frequency was 1024, and temperature was 25 °C.

#### *Skin permeability test*

Skin permeability study was conducted to evaluate the skin permeability of AX (20%) and Evaporation;

EVP (Sol/AX = 9/1, Sol/PEG 2000/AX = 8/1/1), with a standardized preparation of 20 μg/mL of AX, to compare AX (content 20%) suspension and AX-containing particulate formulations (Sol/AX = 9/1 and Sol/PEG 2000/AX = 8/1/1). For pretreatment, frozen skin (− 80 °C) of YUCATAN micropig (YMP, 5-month-old, female, pig number: 95–130) was placed in a refrigerator at 4 °C and thawed before use. After defrosting, subcutaneous fat was removed, and the skin was cut into approximately 2.5 × 2.5 cm circular pieces. The stratum corneum was removed by tape stripping for 30 times, and YMP skin was moisturized with saline solution and stored at 4 °C for 20 h prior to use. Franz-type diffusion cells (Perme Gear, PA, USA; effective penetration area: approximately 0.95 $cm^2$) were used for the skin permeation test, and phosphate-buffered saline (pH 7.4, 1X; Thermo Fisher Scientific Life Technology Japan, Tokyo, Japan) (approximately 9.6 mL) was used as the receiver phase. During the permeation test, the temperature of the receiver phase was maintained at 32 °C, and YMP skin was placed on the Franz-type diffusion cell. The donor phase was filled with 1 mg/mL solution of 20% AX suspension, and various prepared particulate formulations were used as sample reagents.

The permeation of AX in YMP skin was determined using Waters e2695 UV-visible photometer (Waters Japan, Tokyo, Japan) under the following conditions: measurement wavelength 480 nm; column COSMOSIL 5C18AR-II (4.6 mm i.d. × 250 mm; Nacalai Tesque, Kyoto, Japan); column temperature 40 °C; mobile phase acetone/water = 4/1; injection volume 30 μL; retention time of AX was adjusted to approximately 6 min. The detection limit is 0.022 (μg/mL), and the quantification limit is 0.068 (μg/mL).

#### *Fluorescence microscopy*

Fluorescence microscopy was performed using skin segments to visualize skin penetration. The sample was the effective area portion of YMP skin after 24 h of the skin permeability test. YMP skin (approximately 7.0 × 2.0 mm) was placed in a plastic embedding cassette, which was filled with Tissu-Tek O.C.T compound (Sakura Finetek Japan, Tokyo, Japan). Subsequently, the skin was frozen using acetone and dry ice and stored at −80 °C. Frozen samples of 10-μm thickness were cut using LEICA CM3050S (Leica Biosystems, Nussloch, Germany), and frozen slice specimens were prepared. The frozen specimens were observed under an all-in-one fluorescence microscope (BZ-X800; KEYENCE, Osaka, Japan).

## Results and discussion

### Particle size and ZP measurement

We previously reported the formation of novel particulates with Sol/ASC-DP/NOB = 8/1/1 (Inoue et al. 2022). Therefore, we investigated the possibility of microparticle formulation in a ternary system with AX instead of NOB and with Sol/ASC-DP/AX = 8/1/1 (Table 1). To evaluate the stability of the prepared particles, a suspension prepared by dispersion in 0.1 M ascorbic acid solution (0.1 M ASC) and DW was light-shielded, and stability evaluation was conducted for 14 days at 25 °C.

The results showed that in the ternary system Sol/ASC-DP/AX = 8/1/1, the average particle size was d50 = 141.9 ± 0.8 (nm) and ZP was -16.2 ± 0.7 mV (Fig. 1e-1) on day 0 of suspension preparation in DW, compared with d50 = 138.6 ± 2.0 (nm) and ZP = -12.0 ± 0.3 mV, respectively, after storage for 14 days (Fig. 1e-2). In contrast, a sample of Sol/ASC-DP/AX = 8/1/1 dispersed in 0.1 M ASC showed a mean particle size of d50 = 178.0 ± 3.2 (nm) and ZP = 0.3 ± 0.07 mV on day 0 of preparation (Fig. 2e-1), compared with d50 = 241.8 ± 2.4 (nm) and ZP = 1.8 ± 0.2 mV, respectively, after storage for 14 days (Fig. 2e-2). Consequently, in the ternary system Sol/ASC-DP/AX = 8/1/1, no change in the mean particle size was observed from day 0 to day 14 for the sample dispersed in DW. However, the particle size distribution of the sample dispersed in 0.1 M ASC showed a change after storage, and a bimodal distribution of particle size was observed on 14th day of preparation (Fig. 2e-2), indicating heterogeneous mixture because of the admixture of particles with two different size distributions. Therefore, we hypothesized that using PEG, a surfactant, instead of ASC-DP and encapsulating AX in the polymeric micelle core of PEG would prevent particle agglomeration and produce uniform particles. In the present study, we also validated a Sol/AX particulate formulation containing PEG instead of ASC-DP. The samples were prepared at mixed weight ratios (Sol/AX = 9/1 and Sol/PEG 2000, 4000, 20,000/AX = 8/1/1), and particle size distribution and ZP measurements were performed

**Table 1** Particle size and zeta potential (ZP) of Sol/PEG and ASC-DP/AX systems in 0.1 M ascorbic acid solution systems

| Sample | Particle size (nm) | ZP (mV) | PDI |
|---|---|---|---|
| Sol/AX=9/1 | 99.43 ± 2.3 | 1.92 ± 0.14 | 0.114 |
| Sol/PEG2000/AX=8/1/1 | 117.3 ± 0.88 | 2.09 ± 0.17 | 0.123 |
| Sol/PEG4000/AX=8/1/1 | 122.1 ± 0.96 | 2.13 ± 0.24 | 0.133 |
| Sol/PEG20000/AX=8/1/1 | 139.0 ± 0.61 | 1.98 ± 0.12 | 0.143 |
| Sol/ASC-DP/AX=8/1/1 | 178.0 ± 3.2 | 0.307 ± 0.066 | 0.141 |

Results are expressed as mean ± S.D. ($n = 3$)

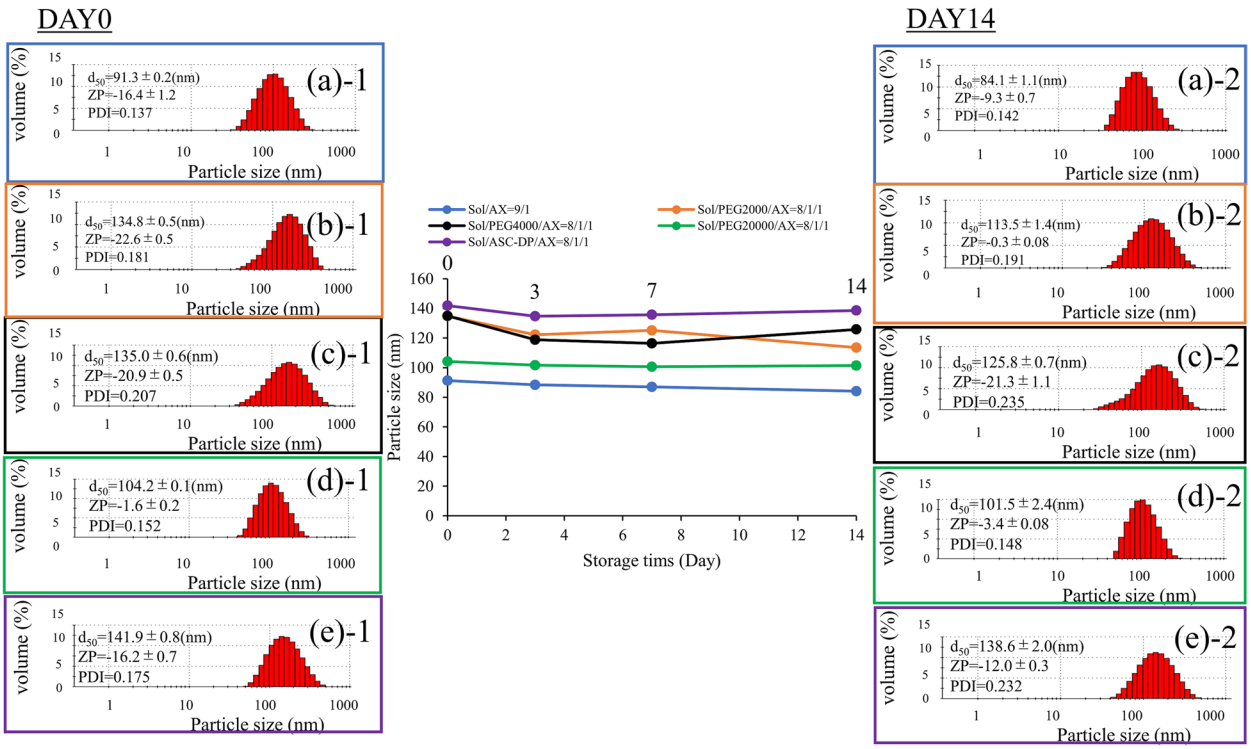


**Fig. 1** Changes in the particle size and zeta potential of Sol/PEG/AX = 8/1/1, Sol/AX = 9/1, and Sol/ASC-DP/AX = 8/1/1 microparticles. Microparticles after storage at 25℃ from day 0 to day 14 in distilled water. Each point represents the mean ± standard deviation ($n = 3$). **a** Sol/AX = 9/1, **b** Sol/PEG 2000/AX = 8/1/1, **c** Sol/PEG 4000/AX = 8/1/1, **d** Sol/PEG 20000/AX = 8/1/1, **e** Sol/ASC-DP/AX = 8/1/1

at 25 °C (Figs. 1 and 2). Sol/AX = 9/1 dispersed in DW showed a sharp distribution with mean particle size d50 = 91.3 ± 0.2 (nm) and ZP = -16.4 ± 1.2 mV on day 0 of preparation (Fig. 1a-1). Moreover, stability evaluation also revealed a sharp distribution of mean particle size d50 = 84.1 ± 1.1 (nm) and ZP = -9.3 ± 0.7 mV after storage for 14 days (Fig. 1a-2). The particle surface charge is an important factor in the evaluation of particle dispersion and stability. It has been reported that particles with ZP greater than ± 30 mV are stable in suspension because of the absence of particle aggregation because of surface charge (Singh and Lillard 2009). On the contrary, high-molecular weight stabilizers, e.g., PEG, are reported to be sufficiently stabilized even with ZP below ± 20 mV (Shaal et al. 2014). Therefore, it can be presumed that Soluplus is relatively stable with a ZP of -16.4 ± 1.2 mV (Fig. 1a-1) at day 0 of the preparation of Sol/AX = 9/1 dispersed in DW, given its high molecular weight and use as a stabilizer (Zeng et al. 2017).

Sol/PEG 2000/AX = 8/1/1 showed a broad particle size distribution with mean particle size d50 = 134.8 ± 0.5 (nm) and ZP = -22.6 ± 0.5 mV on day 0 of preparation (Fig. 1b-1) and d50 = 113.5 ± 1.4 (nm) and ZP = -0.3 ± 0.08 mV, respectively, after storage for 14 days (Fig. 1b-2). This suggests that Sol/PEG 2000/AX = 8/1/1 dispersed in DW exhibits a broad particle size distribution with no variation in the average particle size, indicating considerable agglomeration. We considered that encapsulating AX in the polymeric micelle core improves as the average molecular weight of PEG increases, so we prepared particles the same way with PEG 4000 and 20,000, which have different molecular weights, and evaluated their stability over 14 days. Sol/PEG 4000/AX = 8/1/1 dispersed in DW showed a broad particle size distribution with mean particle size d50 = 135.0 ± 0.6 (nm) and ZP = -20.9 ± 0.5 mV (Fig. 1c-1) on day 0 of preparation. Even after storage for 14 days, a broad particle size distribution was observed with a mean particle size of d50 = 125.8 ± 0.7 (nm) and ZP = -21.3 ± 1.1 mV (Fig. 1c-2). Sol/PEG 20000/AX = 8/1/1 showed a mean particle size of d50 = 104.2 ± 0.1 (nm) and ZP = -1.6 ± 0.2 mV on day 0 of preparation (Fig. 1d-1), and after storage for 14 days, mean particle size was d50 = 101.5 ± 2.4 (nm) and ZP = -3.4 ± 0.08 mV (Fig. 1d-2). Consequently, in the ternary component system using PEG 4000, the ZP was relatively stable at day 0 of preparation (-20.9 ± 0.5 mV) and after 14 days of storage (-21.3 ± 1.1 mV), but broad particle size distribution suggests unstable particles in the system. The ternary

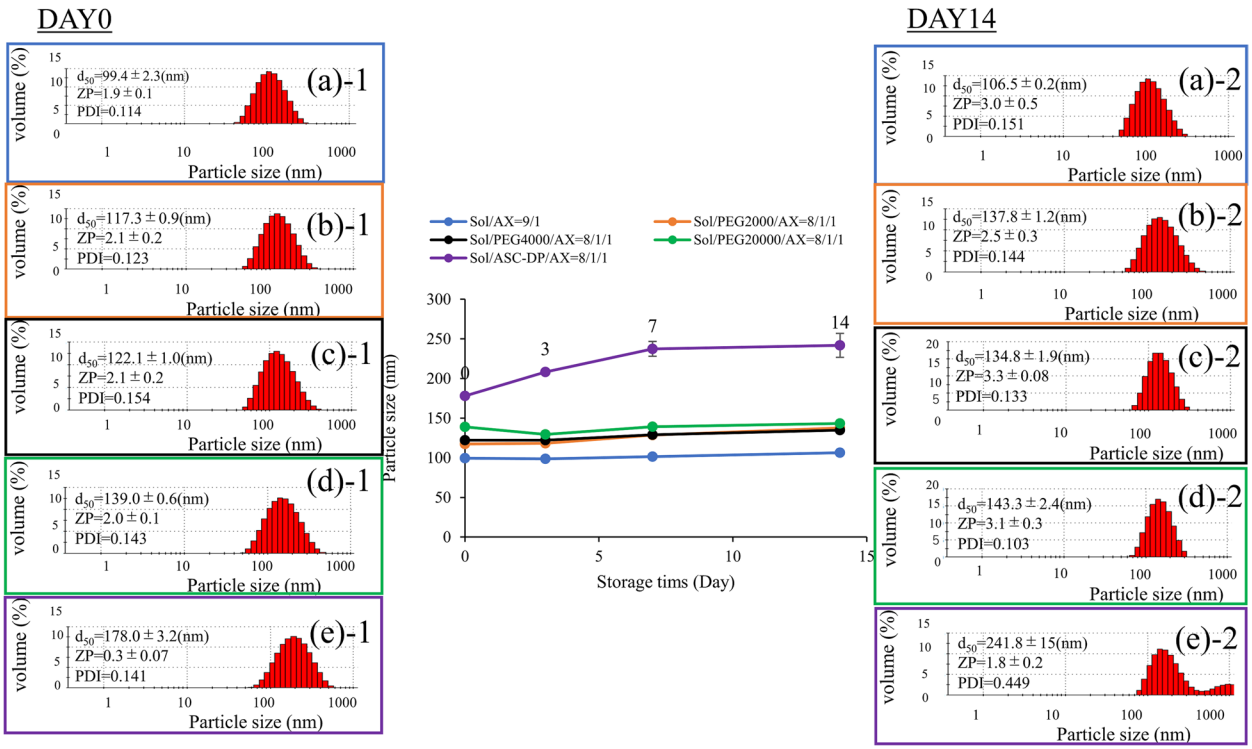


**Fig. 2** Changes in particle size and zeta potential of Sol/PEG/AX = 8/1/1, Sol/AX = 9/1, and Sol/ASC-DP/AX = 8/1/1 microparticles. Microparticles after storage at 25℃ from day 0 to day 14 in 0.1 M ascorbic acid solution. Each point represents the mean ± standard deviation ($n$ = 3). **a** Sol/AX = 9/1, **b** Sol/PEG 2000/AX = 8/1/1, **c** Sol/PEG 4000/AX = 8/1/1, **d** Sol/PEG 20000/AX = 8/1/1, **e** Sol/ASC-DP/AX = 8/1/1

system with PEG 2000 exhibited a steep particle size distribution; however, the particles were considered unstable owing to their low ZPs.

When dispersed in 0.1 M ASC, Sol/PEG 2000/AX = 8/1/1, the average particle size was d50 = 117.3 ± 0.9 (nm) and ZP = 2.1 ± 0.2 mV on day 0 of preparation (Fig. 2b-1), and d50 = 137.8 ± 1.2 (nm) and ZP = 2.5 ± 0.3 mV, respectively, after 14 days of storage (Fig. 2b-1, b-2). The two-component system Sol/AX = 9/1 showed a mean particle size d50 = 99.4 ± 2.3 (nm) and ZP = 1.9 ± 0.1 mV on day 0 of preparation (Fig. 2a-1), and d50 = 106.5 ± 0.2 (nm) and ZP = 3.0 ± 0.5 mV, respectively, after 14 days of storage (Fig. 2a-2). These results suggest that the dispersion in 0.1 M ASC provides a steeper particle size distribution than that of DW, with no change in mean particle size or ZP with the storage period. In contrast, ZP was low, with absolute value of approximately 2–3 mV, that might be attributed to the self-assembly of micelles of Soluplus or polymeric micelle core of PEG, which covered the particle surface and prevented aggregation via the stabilizing effects of various substances. The stability of the particles dispersed in 0.1 M ASC was studied in the same way for ternary systems with PEG 4000 and PEG 20000. Sol/PEG 4000/AX = 8/1/1 showed an average particle size d50 = 122.1 ± 1.0 (nm) and ZP = 2.1 ± 0.2 mV on day 0 of preparation (Fig. 2c-1), and d50 = 34.8 ± 1.9 (nm) and ZP = 3.3 ± 0.08 mV, respectively, after 14 days of storage (Fig. 2c-2). Sol/PEG 2000/AX = 8/1/1 showed a mean particle size d50 = 139.0 ± 0.6 (nm) and ZP = 2.0 ± 0.1 mV on day 0 of preparation (Fig. 2d-1), whereas it was d50 = 143.3 ± 2.4 (nm) and ZP = 3.1 ± 0.3 mV, respectively, after storage for 14 days (Fig. 2d-2). As with PEG 2000, there was no change in the mean particle size or ZP with storage time, and a sharp particle size distribution was obtained. The ZP was approximately 2–3 mV, similar to that of PEG 2000, and we speculated that this was because of the stabilizing effects of Sol or PEG elicited via prevention of aggregation.

When the ternary systems with PEG 2000 and PEG 4000 were dispersed in DW, a broad particle size distribution was obtained, and the particles were considered to exist in an unstable state because of agglomeration. In contrast, when dispersed with 0.1 M ASC, there was no change in mean particle diameter or ZP with the storage period, and a sharp particle size distribution was obtained. Thus, stable fine particles could be obtained in various mixtures of Sol/PEG/AX = 8/1/1 and Sol/AX = 9/1 through dispersion in 0.1 M ASC. Based on these results, colorimetry and fluorescence spectroscopy

measurements were performed to further investigate the stability of AX in the prepared Sol/PEG/AX = 8/1/1 and Sol/AX = 9/1.

### Colorimetry measurement and fluorescence spectroscopy

The samples prepared at various mixture weight ratios were dispersed in DW or 0.1 M ascorbic acid solution (0.1 M ASC), and the stability of AX was evaluated at 25 °C after 14 days of storage using a colorimeter/chromometer and fluorescence spectrophotometer. On day 0 of preparation, Sol/AX = 9/1 hydrated with DW showed a = 26.2 and b = 64.2, indicating a bright orange color (Fig. 3a-1, Table 2). The colorimeter value indicates that the larger the value in positive direction, the higher the intensity of red color, and a negative value is represented by green color. In contrast, the b value indicates that the larger the value in the positive direction, the higher the intensity of yellow color, and a negative b value is represented by blue color. After 14 days of storage, it showed a = -0.4 and b = 2.3 was colorless and transparent (Fig. 3a-2). Sol/PEG 2000/AX = 8/1/1 showed a = 31.9 and b = 73.7 on day 0 (Fig. 3b-1), indicating a bright orange color. After 14 days of storage, it showed a = -0.16 and b = 4.3 and was colorless and clear, as was Sol/AX = 9/1 (Fig. 3b-2). Sol/PEG 4000/AX = 8/1/1 and Sol/PEG 20000/AX = 8/1/1 also showed a = 28.5, 62.7, 20.6, and 49.4, respectively, on day 0 of preparation (Fig. 3d-1) and a bright orange color (Fig. 3c-1). After storage for 14 days, a = -0.32, b = 2.47 (Fig. 3c-2) and a = -0.56, b = 3.98, respectively (Fig. 3d-2), and was colorless and transparent (Fig. 3d-3). Thus, it is considered that the use of DW as a dispersion medium causes the oxidation of AX, resulting in the observed color fading, and AX stability is not maintained.

In contrast, Sol/AX = 9/1 hydrated with 0.1 M ASC showed a = 27.0 and b = 63.6 on day 0 of preparation, showing a bright orange color characteristic of AX (Fig. 4a-1, Table 3). After storage for 14 days, a = 25.8, b = 66.0, and no color fading was observed, showing the same bright orange color (Fig. 4a-2). Sol/PEG 2000/

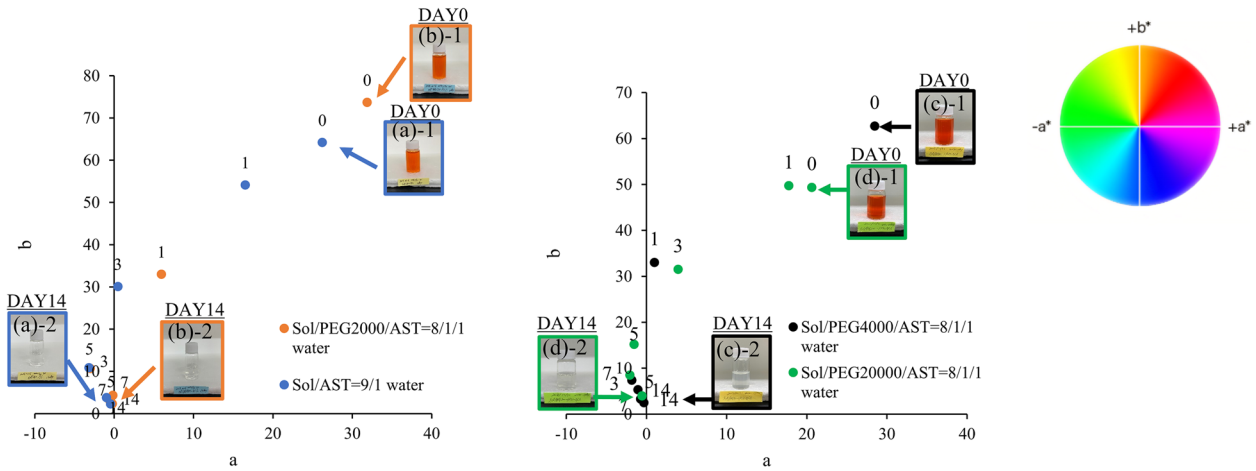


**Fig. 3** Changes in color difference and colorimetric images of Sol/PEG/AX = 8/1/1, Sol/AX = 9/1, and Sol/ASC-DP/AX = 8/1/1 microparticles after storage at 25℃ from day 0 to day 14 in distilled water. **a** Sol/AX = 9/1, **b** Sol/PEG 2000/AX = 8/1/1, **c** Sol/PEG 4000/AX = 8/1/1, **d** Sol/PEG 20000/AX = 8/1/1

**Table 2** Changes in color difference meter various particles after the storage at 25℃ DAY0 to DAY14 in D.W

| Samples | axis | DAY 0 | DAY 1 | DAY 3 | DAY 5 | DAY 7 | DAY 14 |
|---|---|---|---|---|---|---|---|
| Sol/AX =9/1 | a | 26.2 ± 1.0 | 16.5 ± 0.1 | 0.5 ± 0.1 | -3.2 ± 0.1 | -1.0 ± 0.1 | -0.4 ± 0.0 |
| | b | 64.2 ± 2.1 | 54.1 ± 0.1 | 30.1 ± 0.5 | 10.8 ± 0.1 | 3.8 ± 0.1 | 2.3 ± 0.1 |
| Sol/PEG2000/AX =8/1/1 | a | 31.9 ± 0.1 | 6.0 ± 0.1 | -3.0 ± 0.1 | -0.6 ± 0.1 | -0.2 ± 0.1 | -0.2 ± 0.1 |
| | b | 73.7 ± 0.1 | 33.0 ± 0.1 | 10.7 ± 0.1 | 3.1 ± 0.1 | 0.3 ± 0.1 | 4.3 ± 0.1 |
| Sol/PEG4000/AX =8/1/1 | a | 28.5 ± 2.0 | 1.0 ± 0.1 | -1.8 ± 0.1 | -1.1 ± 0.1 | -0.7 ± 0.1 | -0.3 ± 0.1 |
| | b | 62.7 ± 2.9 | 33.0 ± 1.8 | 7.4 ± 0.1 | 5.3 ± 0.1 | 3.3 ± 0.1 | 2.5 ± 0.1 |
| Sol/PEG20000/AX =8/1/1 | a | 20.6 ± 1.5 | 17.8 ± 0.2 | 4.0 ± 0.1 | -1.6 ± 0.1 | -2.1 ± 0.2 | -0.6 ± 0.1 |
| | b | 49.4 ± 3.3 | 49.7 ± 0.2 | 31.5 ± 0.2 | 15.2 ± 0.5 | 8.5 ± 0.6 | 4.0 ± 0.2 |

Results are expressed as mean ± S.D. ($n = 3$)

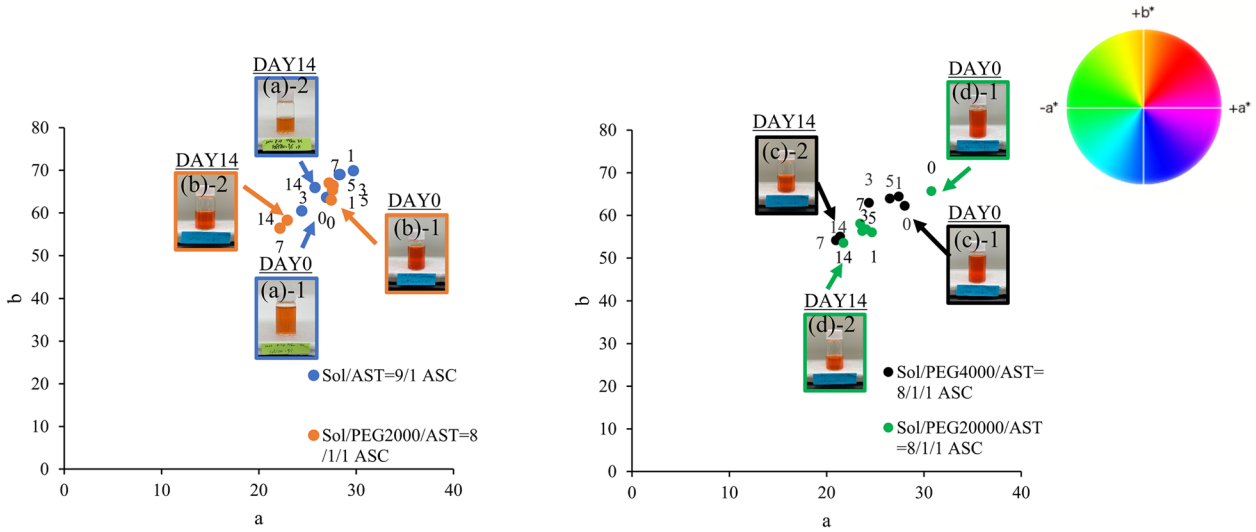


**Fig. 4** Changes in color difference and colorimetric images of Sol/PEG/AX = 8/1/1, Sol/AX = 9/1, and Sol/ASC-DP/AX = 8/1/1 microparticles after storage at 25℃ from day 0 to day 14 in 0.1 M ascorbic acid solution. **a** Sol/AX = 9/1, **b** Sol/PEG 2000/AX = 8/1/1, **c** Sol/PEG 4000/AX = 8/1/1, **d** Sol/PEG 20000/AX = 8/1/1

**Table 3** Changes in color difference meter various particles after the storage at 25℃ DAY0 to DAY14 in D.W. in 0.1 M ascorbic acid solution

| Samples | axis | DAY 0 | DAY 1 | DAY 3 | DAY 5 | DAY 7 | DAY 14 |
|---|---|---|---|---|---|---|---|
| Sol/AX =9/1 | a | 27.0 ± 1.1 | 29.7 ± 0.4 | 24.4 ± 0.8 | 28.3 ± 0.1 | 28.3 ± 0.3 | 25.8 ± 0.6 |
| | b | 63.6 ± 2.2 | 69.9 ± 0.6 | 60.5 ± 2.3 | 69.0 ± 0.1 | 68.9 ± 0.3 | 66.0 ± 1.1 |
| Sol/PEG2000/AX =8/1/1 | a | 27.4 ± 1.7 | 27.6 ± 0.3 | 27.2 ± 0.1 | 27.6 ± 0.7 | 22.2 ± 0.1 | 22.9 ± 0.3 |
| | b | 63.0 ± 3.6 | 65.4 ± 0.5 | 67.0 ± 0.2 | 66.4 ± 1.7 | 56.4 ± 0.2 | 58.3 ± 0.6 |
| Sol/PEG4000/AX =8/1/1 | a | 28.0 ± 1.2 | 27.4 ± 1.1 | 24.4 ± 0.1 | 26.5 ± 0.1 | 21.0 ± 0.6 | 21.4 ± 1.0 |
| | b | 62.2 ± 2.3 | 64.4 ± 2.4 | 62.9 ± 0.1 | 64.0 ± 0.7 | 54.1 ± 1.6 | 55.0 ± 2.4 |
| Sol/PEG20000/AX =8/1/1 | a | 30.8 ± 1.0 | 24.7 ± 1.1 | 23.7 ± 0.4 | 24.1 ± 0.2 | 23.5 ± 0.1 | 21.7 ± 0.1 |
| | b | 65.7 ± 1.6 | 56.0 ± 2.3 | 56.3 ± 0.6 | 56.7 ± 0.2 | 58.1 ± 0.2 | 53.5 ± 0.1 |

Results are expressed as mean ± S.D. ($n = 3$)

AX = 8/1/1 showed a = 27.4 and b = 63.0 on day 0, indicating a bright orange color (Fig. 4b-1). After storage for 14 days, a = 22.9, b = 58.3 (Fig. 4b-2), and the same bright orange color was observed. Sol/PEG 4000/AX = 8/1/1 and Sol/PEG 20000/AX = 8/1/1 also showed a = 28.0, b = 62.2 and a = 30.8, b = 65.7, respectively (Fig. 4d-1) on day 0 of preparation, indicating a bright orange color (Fig. 4c-1). After storage for 14 days, a = 21.4, b = 55.0 (Fig. 4c-2) and a = 21.7, b = 53.5, respectively, showing a gradual decrease in color, but a bright orange color on day 0 of preparation (Fig. 4d-2).

Since AX is a unique red (orange red) dye, in addition to colorimetry, we quantified the emittance and evaluated the storage stability by fluorescence spectroscopy. The fluorescence intensity of Sol/AX = 9/1 dispersed in DW decreased with increasing storage time (Fig. 5a). For Sol/PEG 2000/AX = 8/1/1, different fluorescence intensities were observed on day 0 of preparation and at other storage times (Fig. 5b), suggesting that AX was unstable in the particles. Sol/PEG 4000/AX = 8/1/1 and Sol/PEG 20000/AX = 8/1/1 exhibited different fluorescence intensities at different storage times (Fig. 5c, d). Irregular fluorescence spectral transitions were observed in various mixtures dispersed in DW, suggesting instability of AX in particulate form. On the contrary, Sol/AX = 9/1 dispersed in 0.1 M ASC showed no change in fluorescence intensity with a peak at approximately 678–680 nm (Fig. 6a), and no significant change in fluorescence intensity with storage time was observed for Sol/PEG 2000, 4000, and 20,000/AX = 8/1/1 (Fig. 6b, c, d). This suggests that 0.1 M ASC as a dispersion medium maintains the stability of AX in particulate form. The stability evaluation results after storage for 14 days revealed color fading in various mixtures dispersed in DW and fluctuations in

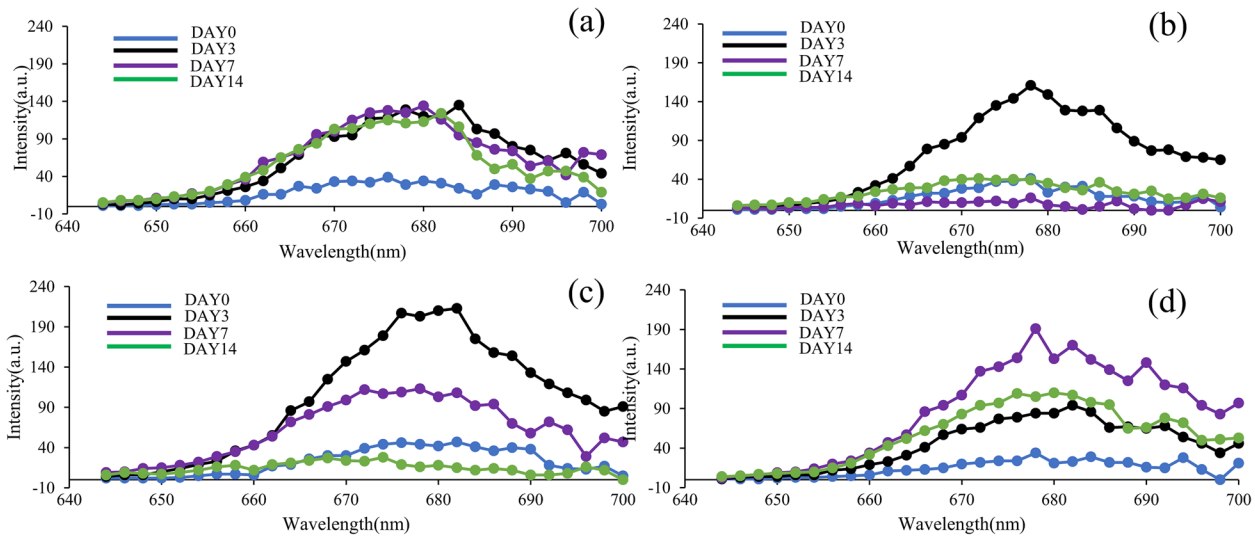


**Fig. 5** Changes in fluorescence spectral measurements of Sol/PEG/AX = 8/1/1, Sol/AX = 9/1, and Sol/ASC-DP/AX = 8/1/1 microparticles after storage at 25℃ from day 0 to day 14 in distilled water. **a** Sol/AX = 9/1, **b** Sol/PEG 2000/AX = 8/1/1, **c** Sol/PEG 4000/AX = 8/1/1, **d** Sol/PEG 20000/AX = 8/1/1

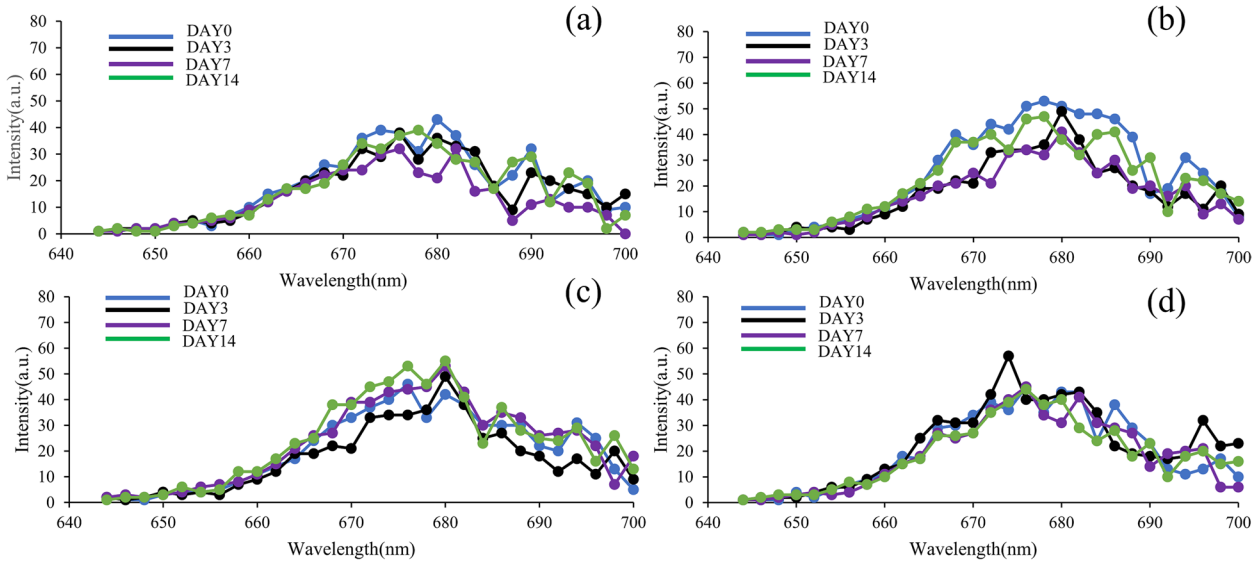


**Fig. 6** Changes in fluorescence spectral measurements of microparticles. Changes in fluorescence spectral measurements of Sol/PEG/AX = 8/1/1, Sol/AX = 9/1, and Sol/ASC-DP/AX = 8/1/1 microparticles after storage at 25℃ from day 0 to day 14 in 0.1 M ascorbic acid solution. **a** Sol/AX = 9/1, **b** Sol/PEG 2000/AX = 8/1/1, **c** Sol/PEG 4000/AX = 8/1/1, **d** Sol/PEG 20000/AX = 8/1/1

fluorescence intensities, suggesting that AX particulates using DW as dispersion medium are unstable. However, no significant color fading or fluctuations in fluorescence intensity were observed immediately after the preparation of various mixtures using 0.1 M ASC as dispersion medium, suggesting the stability of AX particles. In addition to Sol/AX = 9/1, AX particles were stable with PEG 2000, 4000, and 20,000. No significant changes were observed in the particle size distribution, ZP, and fluorescence intensity of samples with 0.1 M ASC as dispersion medium. Therefore, in this study, we used Sol/PEG 2000/AX = 8/1/1 and Sol/AX = 9/1 with 0.1 M ASC as dispersion medium as model formulations for further experiments.

### Singlet oxygen scavenging activity

The antioxidant capacity of AX against highly toxic singlet oxygen is approximately 40 times higher than that of

β-carotene and 550 times higher than that of vitamin E (Shimidzu et al. 1996). Therefore, we measured the singlet oxygen scavenging ability to evaluate the antioxidant capacity of AX in the prepared particulate form. Sol/AX = 9/1 dispersed in 0.1 M ASC showed 97.6% singlet oxygen scavenging capacity, whereas Sol/PEG 2000/AX = 8/1/1, in which PEG 2000 was added to the two-component system, showed singlet oxygen scavenging capacity of 96.3% (Table 4). AX is believed to exert its antioxidant effects on the hydroxy and ketone groups at both ends and on the central conjugated polyene chain (Goto et al. 2001). In this study, any sample dispersed in 0.1 M ASC showed a singlet oxygen scavenging capacity of 96% or higher, suggesting that the antioxidant capacity of the prepared particulates is excellent. In contrast, for Sol/AX = 9/1 hydrated with DW, singlet oxygen scavenging capacity was 12.9% (Table 4). The 0.1 M ASC content did not cause any change in the color of the prepared particles. On the other hand, the Singlet oxygen scavenging activity showed a decrease in antioxidant effect as the color faded with the storage period of the particles. We speculate that the double bond is dissociated in the structure of AX. Therefore, it is supposed that 0.1 M ASC contributes to the retention of the antioxidant capacity of AX particulates and can be used as a dispersion medium.

### TEM

In particle size distribution/ZP measurements and fluorescence spectroscopy, various mixtures with 0.1 M ASC as a dispersion medium confirmed to have stable particles. Therefore, TEM measurements were performed to confirm the shape and particle size distribution of AX particles using suspensions of Sol/AX = 9/1 and Sol/PEG 2000/AX = 8/1/1 dispersed in 0.1 M ASC as model formulations. Sol/AX = 9/1 showed particles of approximately 100 nm (Fig. 7a), and Sol/PEG 2000/AX = 8/1/1 showed particles of approximately 150 nm (Fig. 7b), which is consistent with the results of particle size distribution measurement. The shape of each Sol/PEG 2000/AX = 8/1/1 particle was circular; however, an irregular structure was

**Table 4** Singlet oxygen scavenging ability measurement of Sol/PEG and ASC-DP/AX systems in 0.1 M ascorbic acid solution systems

| Sample | $^1O_2$ Erasure rate | Intensity |
|---|---|---|
| Sol/AX=9/1 D.W. | 12.9% | 27.14 ± 1.12 |
| Sol/AX=9/1 0.1M ASC | 97.6% | 1.87 ± 0.48 |
| Sol/PEG2000/AX=8/1/1 0.1M ASC | 96.3% | 2.92 ± 0.07 |
| Rose Bengal 200μM（50% EtOH) | - | 79.51 ± 6.35 |

※Positive control: L-Histidine 98.37%

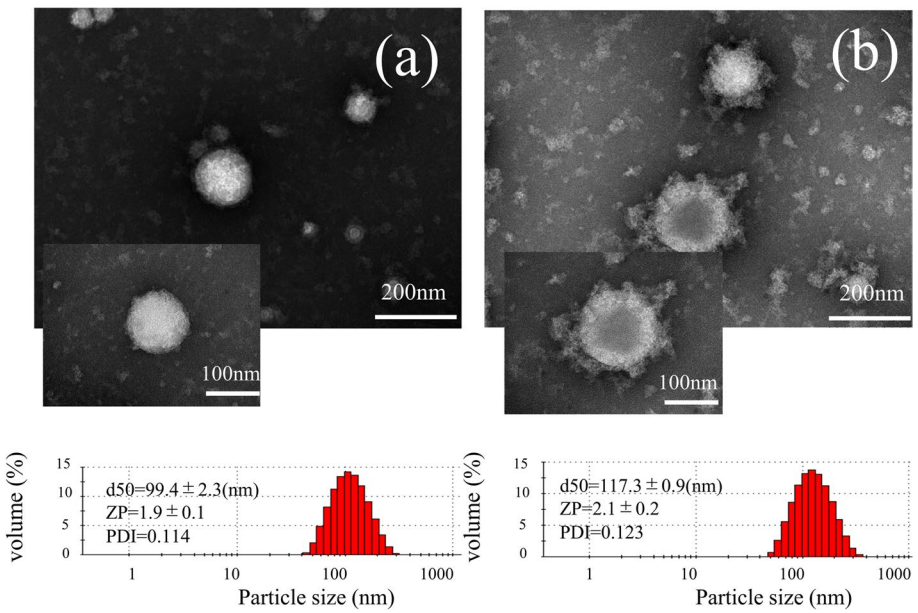


**Fig. 7** TEM images of particles in 0.1 M ASC. **a** Sol/AST = 9/1, **b** Sol/PEG 2000/AST = 8/1/1

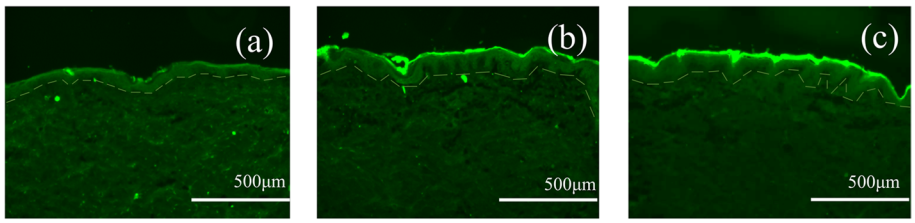


**Fig. 8** Fluorescence microscopy images of the epidermal side of YMP skin. **a** 20% AX, **b** EVP (Sol/AX = 9/1), **c** EVP (Sol/PEG 2000/AX = 8/1/1). × 10 (**a**, **b**, **c**). Bar: border with epidermis

observed around the central core (Fig. 7b). PEG can coat particle surfaces and prevent particle aggregation, thereby contributing to particle stability (Jung et al. 2016; Rahme and Dagher 2019). Therefore, we speculate that PEG contributes to the stability of AX particulates.

### Skin permeability test and fluorescence microscopy observations

Skin permeability studies were performed for suspensions of 20% AX and EVP (Sol/AX = 9/1 and Sol/PEG 2000/AX = 8/1/1). The porcine skin permeability studies using HPLC at 1, 3, 6, and 24 h did not confirm the skin permeation of AX, although quantification was performed using the receiver solution. Therefore, we examined whether AX remained in the skin by homogenizing the effective area of the porcine skin 24 h after the skin permeability test. However, skin permeation was not confirmed by quantifying each sample using homogenized porcine skin. Therefore, to verify the skin condition and permeability of AX, frozen sections were prepared from YMP skin 24 h after the skin permeability test and observed under a fluorescence microscope. The fluorescence of AX was measured at approximately 480 nm

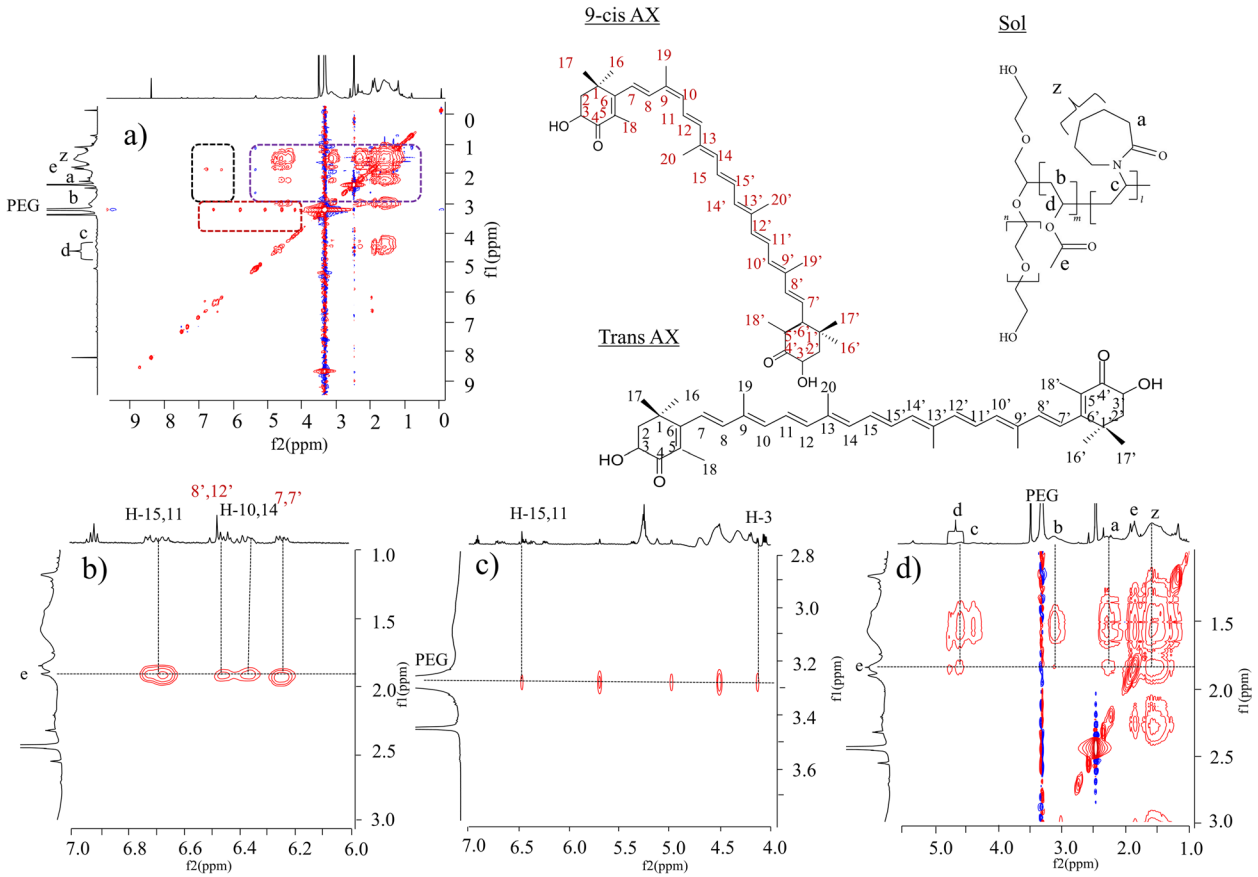


**Fig. 9** $^{1}$H-$^{1}$H NOESY NMR spectra of EVP (Sol/AX = 9/1) in DMSO-$d_6$. **a** f1 is 0–9 ppm, f2 is 0–9 ppm, **b** f1 is 6–7 ppm, f2 is 1–3 ppm, **c** f1 is 4–7 ppm, f2 is 2.8–3-3.8 ppm, **d** f1 is 1–7 ppm, f2 is 1–3 ppm

(Wang et al. 2021). AX luminescence from 20% AX suspension was observed in the keratin (Fig. 8a).

In Sol/AX = 9/1 with 0.1 M ASC, AX luminescence was also observed in the stratum corneum (Fig. 8b), but interestingly, in Sol/PEG 2000/AX = 8/1/1, it was not confined to the stratum corneum but slightly penetrated into the epidermis (Fig. 8c). PEG is a hydrophilic surfactant suitable as a penetration enhancer in topical dermatological preparations (Jang et al. 2015). Surfactants play a bridging role by adsorbing at the interface of inherently immiscible substances. There are lipophilic and hydrophilic areas in the skin; therefore, penetration into the stratum corneum is likely to facilitate this process. Therefore, because slight permeability was observed with the addition of PEG, a surfactant, to the Sol/PEG 2000/AX = 8/1/1, it was inferred that PEG contributed to the improved skin permeation of AX. Therefore, we believe that Sol/PEG 2000/AX = 8/1/1 could be a useful formulation for skin adaptation.

### $^{1}$H-$^{1}$H NOESY NMR experiments

The formation of stable particles was confirmed for Sol/AX = 9/1 and Sol/PEG 2000/AX = 8/1/1 dispersed in 0.1 M ASC. This suggests that intermolecular interactions occurred in the solution. Therefore, to investigate the intermolecular interactions in solution, we performed $^{1}$H-$^{1}$H NOESY NMR spectroscopy. DMSO-$d_6$ was used as NMR solvent, and the attribution of Sol was taken from that reported by Sofroniou et al. (2022), AX was taken from that reported by Wang et al. (2021), and ASC was taken from that reported by Bourafai-Aziez et al. (2022). Initially, these interactions were evaluated using a binary system (Sol/AX = 9/1) (Fig. 9). In EVP (Sol/AX = 9/1) using DMSO as dispersion medium, the interaction between Sol-derived methyl group e (1.8 ~ 2.0 ppm) and AX-derived CH groups H-15,11 (6.7–6.8 ppm), 8',12' (6.4 ~ 6.5 ppm), H-10,14 (6.4 ~ 6.5 ppm), and 7,7' (6.2 ~ 6.3 ppm) (Fig. 9b). Cross peaks were also observed for the PEG backbone of Sol (3.6 ppm) and the CH groups H-15,11 (6.7 ~ 6.8 ppm) and H-13 (4.3 ppm) of AX (Fig. 9c). Interactions were also observed between the methyl group e derived from Sol (1.8 ~ 2.0 ppm) and the 7-membered rings z (1.5 ~ 1.8 ppm), a (2.2 ~ 2.4 ppm), b (3.1 ~ 3.2 ppm), and d (4.6 ~ 4.8 ppm) derived from Sol (Fig. 9d).

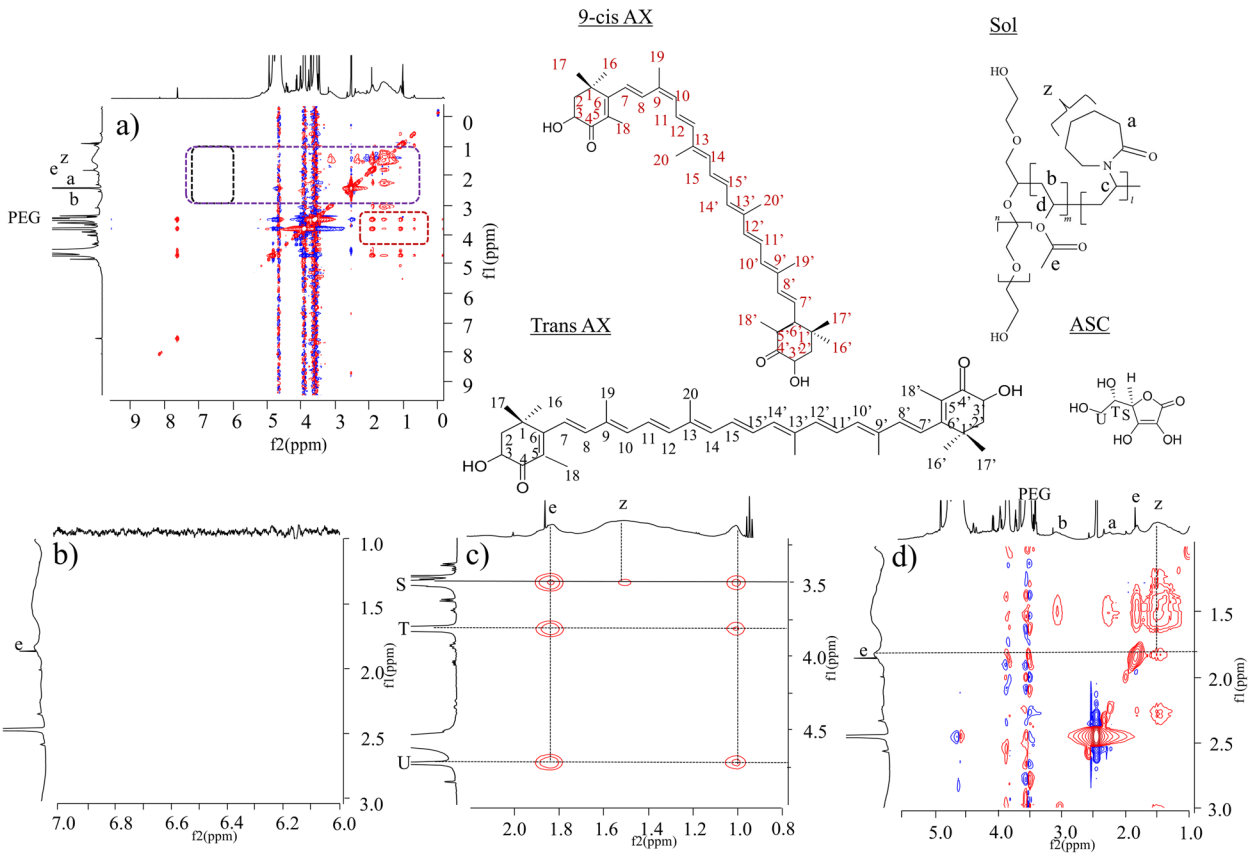


**Fig. 10** $^{1}$H-$^{1}$H NOESY NMR spectra of EVP (Sol/AX = 9/1) in 0.1 M ASC + DMSO. **a** f1 is 0–9 ppm, f2 is 0–9 ppm, **b** f1 is 6–7 ppm, f2 is 1–3 ppm, **c** f1 is 4–7 ppm, f2 is 2.8–3–3.8 ppm, **d** f1 is 1–7 ppm, f2 is 1–3 ppm

Further, EVP (Sol/AX = 9/1) dispersed in 0.1 M ASC and a small amount of DMSO-$d_6$ (Fig. 10) showed the Sol-derived methyl group e (1.8 ~ 2.0 ppm) and AX-derived CH groups H-15,11 (6.7 ~ 6.8 ppm), 8',12' (6.4 ~ 6.5 ppm), H-10,14 (6.4 ~ 6.5 ppm) and 7,7' (6.2 ~ 6.3 ppm) (Fig. 10b). Interestingly, new cross peaks were observed between the methyl group e of Sol (1.8 ~ 2.0 ppm), the 7-membered ring z of Sol (1.5 ~ 1.8 ppm), the 5-membered ring S of ASC (3.5 ~ 3.6 ppm), the CH group T (3.8 ~ 3.9 ppm), and the CH group U (4.7 ppm) (Fig. 10c). In addition, an interaction was observed between the methyl group e of Sol (1.8 ~ 2.0 ppm) and the 7-membered ring z of Sol (1.5 ~ 1.8 ppm) (Fig. 10c). These results suggest that intermolecular interactions may occur between Sol/AX and PEG/AX with Sol/AX = 9/1 using DMSO as dispersion medium. Moreover, it was suggested that intermolecular interactions may have occurred between Sol/AX with 0.1 M ASC and Sol/AX = 9/1 particles with DMSO alone. In addition, few intermolecular interactions in Sol/AX and the disappearance of few interactions in Sol/Sol were suggested. This suggests that the interaction in Sol/ASC and the disappearance of few intermolecular interactions in Sol/AX might have contributed to AX stabilization.

Subsequently, the interactions in a three-component system (Sol/PEG 2000/AX = 8/1/1) were evaluated (Fig. 11). Similar to EVP (Sol/AX = 9/1), interactions were observed between the methyl groups e (1.8 ~ 2.0 ppm) of Sol and CH groups H-15,11 (6.7 ~ 6.8 ppm) of AX, 8',12' (6.4 ~ 6.5 ppm), H-10,14 (6.4 ~ 6.5 ppm), and 7,7' (6.2 ~ 6.3 ppm) in Sol/PEG 2000/AX = 8/1/1 with DMSO as dispersion medium (Fig. 11b). In addition, cross peaks were observed for the PEG backbone of Sol (3.6 ppm) and the CH groups H-15,11 (6.7 ~ 6.8 ppm) and H-13 (4.3 ppm) of AX (Fig. 11c). Interactions were also observed between the methyl group e of Sol (1.8 ~ 2.0 ppm) and the 7-membered rings z (1.5 ~ 1.8 ppm), a (2.2 ~ 2.4 ppm), b (3.1 ~ 3.2 ppm), and d (4.6 ~ 4.8 ppm) of Sol (Fig. 11d). In contrast, in EVP (Sol/PEG 2000/AX = 8/1/1) dispersed in 0.1 M ASC and a small amount of DMSO-d6 (Fig. 12), the interactions were observed between the methyl group e (1.8 ~ 2.0 ppm) of Sol and CH groups H-15,11 of AX (6.7 ~ 6.8 ppm), 8',12' (6.4 ~ 6.5 ppm), H-10,14 (6.4 ~ 6.5 ppm), and 7,7' (6.2 ~ 6.3 ppm) (Fig. 12b). Similar to EVP (Sol/AX = 9/1), new cross peaks were observed for the methyl group e of Sol (1.8 ~ 2.0 ppm),

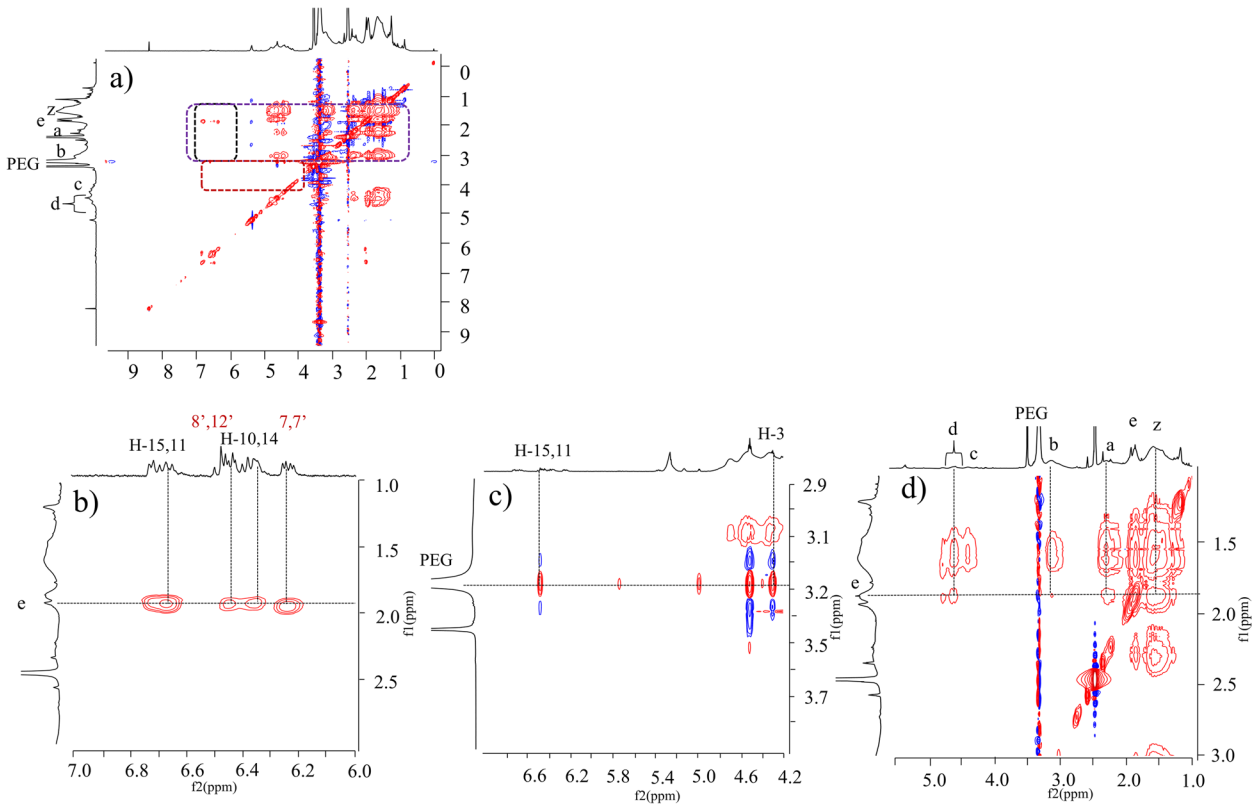


**Fig. 11** $^{1}$H-$^{1}$H NOESY NMR spectra of EVP (Sol/PEG 2000/AX = 8/1/1) in DMSO. **a** f1 is 0–9 ppm, f2 is 0–9 ppm, **b** f1 is 6–7 ppm, f2 is 1–3 ppm, **c** f1 is 4.2–6.8 ppm, f2 is 2.9–3-3.9 ppm, **d** f1 is 1–7 ppm, f2 is 1–3 ppm

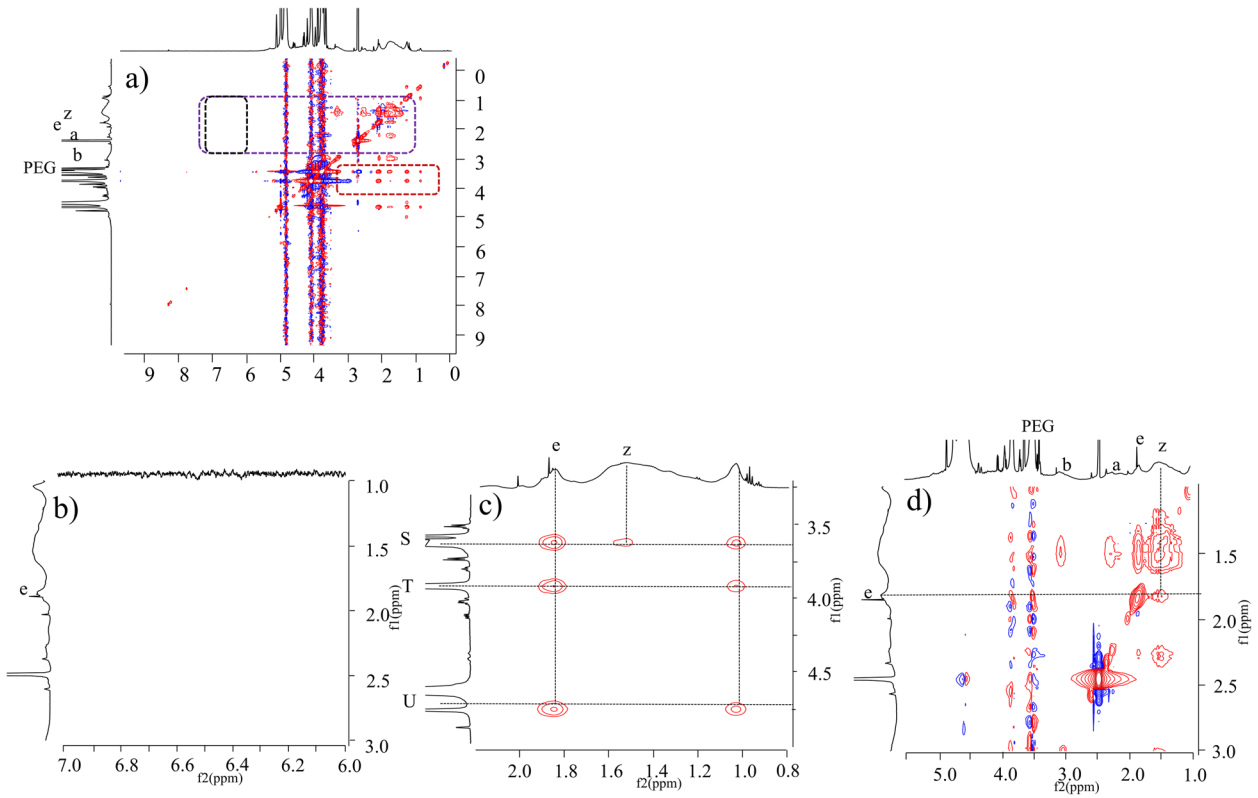


**Fig. 12** $^{1}$H-$^{1}$H NOESY NMR spectra of EVP (Sol/PEG 2000/AX = 8/1/1) in 0.1 M ASC + DMSO. **a** f1 is 0–9 ppm, f2 is 0–9 ppm, **b** f1 is 6–7 ppm, f2 is 1–3 ppm, **c** f1 is 4–7 ppm, f2 is 2.8–3–3.8 ppm, **d** f1 is 1–7 ppm, f2 is 1–3

7-membered ring z of Sol (1.5 ~ 1.8 ppm), 5-membered ring S of ASC (3.5 ~ 3.6 ppm), CH group T (3.8 ~ 3.9 ppm), and CH group U (4.7 ppm) (Fig. 12b, c). Also, an interaction was observed between the methyl group e of Sol (1.8 ~ 2.0 ppm) and the 7-membered ring z of Sol (1.5 ~ 1.8 ppm) (Fig. 12d).

In EVP (Sol/PEG 2000/AX = 8/1/1) with 0.1 M ASC, a peak similar to EVP (Sol/AX = 9/1) was observed. Because of the presence of PEG in Sol, it was not possible to distinguish the PEG peak in Sol from the PEG peak in PEG 2000. The addition of 0.1 M ASC altered the Sol/AX interaction, suggesting that 0.1 M ASC acted as an oxidant for some double bonds in AX, maintaining AX stability and contributing to stable particulate formation and skin permeability.

Thus, NMR spectral measurements of both Sol/AX = 9/1 and Sol/PEG/AX = 8/1/1 not only revealed the interactions related to particle formation but also elucidated how ASC plays a role in the retention of the antioxidant effect of AX. This supports the retention of singlet oxygen at Sol/AX = 9/1 or Sol/PEG/AX = 8/1/1 and the data from colorimetric measurements. Thus, ASC is necessary for AX formulation as it allows the formation of stable particles of AX. The findings provide novel information about the interaction between ASC and AX and the mechanism of action of ASC related to the antioxidant effect of AX.

Finally, as a limitation of the study, we are of the belief that the skin permeability test was conducted in this study using HPLC, but could not be sufficiently quantified because it was below the detection limit. In addition to this, the study has been studied using the three components of Sol/PEG 2000/AX, but should be studied using other additive components in the future.

## Conclusions

Novel AX particulates were successfully formulated with Sol/AX = 9/1 (approximately 100 nm in size) using the hydration method and with Sol/PEG 2000/AX = 8/1/1 (approximately 125 nm in size). In each component system using DW as dispersion medium, a decrease in fluorescence intensity and color fading were observed after storage for several days. However, in case of 0.1 M ASC as dispersion medium, no significant change in fluorescence intensity was observed immediately after preparation, and a bright orange color was consistently observed, indicating the formation and maintenance of stable particulates. NMR

spectral measurements suggested the loss of some cis-trans double bond interactions of AX in Sol/AX sample with 0.1 M ASC as dispersion medium. This suggests that 0.1 M ASC acts as an oxidant for the double bond of AX, leading to the formation of stable new particles with Sol/PEG 2000/AX = 8/1/1 and Sol/AX = 9/1. In addition, skin permeation test and fluorescence microscopy observations showed that although no skin permeation was observed, slight penetration into the skin was observed for Sol/PEG 2000/AX = 8/1/1 compared with that for Sol/AX = 9/1. In conclusion, stable new particulates were formed with Sol/PEG 2000/AX = 8/1/1, which may contribute to the expansion of AX applications in many fields, including skincare, cosmetics, food, and pharmaceuticals.

**Abbreviations**

| | |
|---|---|
| AX | Astaxanthin |
| Sol | Soluplus |
| PEG | Polyethylene glycol |
| ASC-DP | L-Ascorbyl 2,6-dipalmitate |
| DW | Distilled water |
| ASC | Ascorbic acid |
| EVP | Evaporation |
| ZP | Zeta potential |
| NMR | Nuclear magnetic resonance |
| NOESY | Nuclear overhauser effect spectroscopy |
| YMP | Yucatan micropig |
| HPLC | High-performance liquid chromatography |
| DDS | Drug delivery system |

**Authors' contributions**

Conceptualization: Miyu Ai, Risa Kanai, Hiroaki Todo, Yutaka Inoue; Methodology: Miyu Ai, Risa Kanai, Hiroaki Todo, Junki Tomita, Takashi Tanikawa, Yutaka Inoue; Formal analysis and investigation: Miyu Ai, Risa Kanai, Hiroaki Todo, Junki Tomita, Takashi Tanikawa, Yutaka Inoue; Writing – original draft preparation: Miyu Ai, Hiroaki Todo, Junki Tomita, Yutaka Inoue; Writing – review and editing: Miyu Ai, Hiroaki Todo, Takashi Tanikawa, Yutaka Inoue; Funding acquisition: Miyu Ai, Risa Kanai, Hiroaki Todo, Junki Tomita, Yutaka Inoue; Resources: Miyu Ai, Yutaka Inoue, Hiroaki Todo; Supervision: Miyu Ai, Risa Kanai, Hiroaki Todo, Junki Tomita, Yutaka Inoue.

## Declarations

**Availability of data and materials**

You may consider replacing this with: Data sharing is not applicable to this article as no datasets were generated or analyzed during the current study.

**Competing interests**

The authors declare that they have no competing interests.

**Funding**

Not applicable.

**Acknowledgements**

The authors wish to thank Junki Tomita of the Instrument Analysis Center at Josai University for his helpful advice regarding NMR measurements. We would like to express our sincere gratitude to the members of the Safety and Analysis Laboratory at KOSÉ Co., Ltd. for their helpful advice and cooperation regarding TEM measurements and singlet oxygen scavenging ability measurements.

**Ethics approval and consent to participate**

Not applicable.

**Author details**

[1]Laboratory of Nutri-Pharmacotherapeutics Management, Faculty of Pharmacy and Pharmaceutical Sciences, Josai University, 1-1 Keyakidai, Sakado, Saitama 3500295, Japan. [2]Laboratory of Pharmaceutics and Cosmeceutics, Faculty of Pharmacy and Pharmaceutical Sciences, Josai University, 1-1 Keyakidai, Sakado, Saitama 3500295, Japan. [3]Instrument Analysis Center, Josai University, 1-1 Keyakidai, Sakado, Saitama 3500295, Japan.

Received: 31 May 2024 Accepted: 6 August 2024
Published online: 02 September 2024

**References**

Alves A, Sousa E, Kijjoa A, Pinto M (2020) Marine-derived compounds with potential use as cosmeceuticals and nutricosmetics. Molecules 25(11):2536. https://doi.org/10.3390/molecules25112536

Barenholz Y (2012) Doxil—the first FDA-approved nano-drug: lessons learned. J Control Release 160(2):117–134. https://doi.org/10.1016/j.jconrel.2012.03.020

Bourafai-Aziez A, Jacob D, Charpentier G, Cassin E, Rousselot G, Moing A, Deborde C (2022) Development, validation, and use of 1H-NMR spectroscopy for evaluating the quality of Acerola-based food supplements and quantifying ascorbic acid. Molecules 27(17):51614. https://doi.org/10.3390/molecules27175614

Chang MX, Xiong F (2020) Astaxanthin and its effects in inflammatory responses and inflammation-associated diseases: Recent advances and future directions. Molecules 25(22):5342. https://doi.org/10.3390/molecules25225342

Davinelli S, Nielsen ME, Scapagnini G (2018) Astaxanthin in skin health, repair, and disease: a comprehensive review. Nutrients 10(4):522. https://doi.org/10.3390/nu10040522

Goto S, Kogure K, Abe K, Kimata Y, Kitahama K, Yamashita E, Terada H (2001) Efficient radical trapping at the surface and inside the phosphor lipids membrane is responsible for highly potent antioxidative activity of the carotenoid astaxanthin. Biochem Biophys Acta 1521(2):251–258. https://doi.org/10.1016/s0005-2736(01)00326-1

Gulzar S, Benjakul S (2020) Characteristics and storage stability of nanoliposomes loaded with shrimp oil as affected by ultrasonication and microfluidization. Food Chem 310:125916. https://doi.org/10.1016/j.foodchem.2019.125916

Ibrahim M, Ramadan E, Elsadek N, Emam SE, Shimizu T, Ando H, Ishima Y, Elgarhy OH, Sarhan HA, Hussein AK, Ishida T (2022) Polyethylene glycol (PEG): the nature, immunogenicity, and role in the hypersensitivity of PEGylated products. J Control Release 351:215–230. https://doi.org/10.1016/j.jconrel.2022.09.031

Inoue Y, Hibino M, Murata I, Kanamoto I (2017) A nanocarrier skin-targeted drug delivery system using an ascorbic acid derivative. Pharm Res 35:1. https://doi.org/10.1007/s11095-017-2311-3

Inoue Y, Ishizawa M, Itakura S, Tanikawa T, Todo H (2022) Verification of nanoparticle formation, skin permeation, and apoptosis using nobiletin as a methoxyfavonoid derivative. AAPS Open 8:17. https://doi.org/10.1186/s41120-022-00065-2

Jang HJ, Shin CY, Kim KB (2015) Safety evaluation of polyethylene glycol (PEG) compounds for cosmetic use. Toxicol Res 31:105–136. https://doi.org/10.5487/TR.2015.31.2.105

Jung J, Raghavendra G. M, Kim D, Seo J (2016) One-step synthesis of starch-silver nanoparticle solution and its application to antibacterial paper coating. Int J Biol Macromol 107(Pt B):2285–2290. https://doi.org/10.1016/j.ijbiomac.2017.10.108

Kim S, Cho E, Yoo J, Cho E, Choi SJ, Son SM, Lee JM, In MJ, Kim DC, Kim JH, Chae HJ (2010) β-CD-mediated encapsulation enhanced stability and solubility of astaxanthin. J Korean Soc Appl Biol Chem 53:559–565. https://doi.org/10.3839/jksabc.2010.086

Kohandel Z, Farkhondeh T, Aschner M, Pourbagher-Shahri AM, Samarghandian S (2015) Anti-inflammatory action of astaxanthin and its use in the treatment of various diseases. Biomed Pharmacother 145:112179. https://doi.org/10.1016/j.biopha.2021.112179

Kosaka Y, Saeki T, Takano T, Aruga T, Yamashita T, Masuda N, Koibuchi Y, Osaki A, Watanabe J, Suzuki R (2022) Multicenter randomized open-label phase II clinical study comparing outcomes of NK105 and paclitaxel in advanced

or recurrent breast cancer. Int J Nanomedicine 17:4567–4578. https://doi.org/10.2147/IJN.S372477
Landon R, Gueguen V, Petite H, Letourneur D, Pavon-Djavid G, Anagnostou F (2020) Impact of astaxanthin on diabetes pathogenesis and chronic complications. Mar Drugs 18(7):357. https://doi.org/10.3390/md18070357
Martinez-Alvarez O, Calvo MM, Gomez-Estaca J (2020) Recent advances in astaxanthin micro/nanoencapsulation to improve its stability and functionality as a food ingredient. Mar Drugs 18(8):406. https://doi.org/10.3390/md18080406
Mishra PR, Shaal LA, Müller RH, Keck CM (2009) Production and characterization of Hesperetin nanosuspensions for dermal delivery. Int J Pharm 371(1–2):182–189. https://doi.org/10.1016/j.ijpharm.2008.12.030
Odeberg JM, Lignell A, Pettersson A, Höglund P (2003) Oral bioavailability of the antioxidant astaxanthin in humans is enhanced by incorporation of lipid based formulations. Eur J Pharm Sci 19(4):299–304. https://doi.org/10.1016/s0928-0987(03)00135-0
Oku N (2017) Innovations in liposomal DDS technology and its application for the treatment of various diseases. Biol Pharm Bull 40(2):119–127. https://doi.org/10.1248/bpb.b16-00857
Onoue S, Yamada S, Chan HK (2014) Nanodrugs: pharmacokinetics and safety. Int J Nanomedicine 9:1025–1037. https://doi.org/10.2147/IJN.S38378
Özdemir C, Güner A (2007) Solubility profiles of poly (ethylene glycol)/solvent systems, I: qualitative comparison of solubility parameter approaches. Eur Polym J 43(7):3068–3093. https://doi.org/10.1016/j.eurpolymj.2007.02.022
Patil AD, Kasabe PJ, Dandge PB (2022) Pharmaceutical and nutraceutical potential of natural bioactive pigment: astaxanthin. Nat Prod Bioprospect 12:25. https://doi.org/10.1007/s13659-022-00347-y
Pignatello R, Corsaro R, Bonaccorso A, Zingale E, Carbone C, Musumeci T (2022) Soluplus® polymeric nanomicelles improve solubility of BCS-class II drugs. Drug Deliv Transl Res 12:1991–2006. https://doi.org/10.1007/s13346-022-01182-x
Rahme K, Dagher N (2019) Chemistry routes for copolymer synthesis containing PEG for targeting, imaging, and drug delivery purposes. Pharmaceutics 11(7):327. https://doi.org/10.3390/pharmaceutics11070327
Ren Y, Deng J, Huang J, Wu Z, Yi L, Bi Y, Chen F (2021) Using green alga *Haematococcus pluvialis* for astaxanthin and lipid co-production: advances and outlook. Bioresour Technol 340:125736. https://doi.org/10.1016/j.biortech.2021.125736
Sekikawa T, Kizawa Y, Li Y, Miura N (2023) Effects of diet containing astaxanthin on visual function in healthy individuals: a randomized, double-blind, placebo-controlled, parallel study. J Clin Biochem Nutr 72(1):74–81. https://doi.org/10.3164/jcbn.22-65
Shaal LA, Mishra PR, Müller RH, Keck CM (2014) Nanosuspensions of hesperetin: preparation and characterization. Pharmazie 69(3):173–82. https://doi.org/10.1691/ph.2014.3032
Shimidzu N, Goto M, Miki W (1996) Carotenoids as singlet oxygen quenchers in marine organisms. Fish Sci 62:134–137. https://doi.org/10.2331/fishsci.62.134
Singh R, Lillard JW Jr (2009) Nanoparticle-based targeted drug delivery. Exp Mol Pathol 89(3):215–223. https://doi.org/10.1016/j.yexmp.2008.12.004
Sofroniou C, Baglioni M, Mamusa M, Resta C, Doutch J, Smets J, Bagliomi P (2022) Self-assembly of Solplus in aqueous solutions: characterization and prospectives on perfume encapsulation. ACS Appl Mater Interfaces 14(12):14791–14804. https://doi.org/10.1021/acsami.2c01087
Suk JS, Xu Q, Kim N, Hanes J, Ensigh LM (2016) PEGylation as a strategy for improving nanoparticle-based drug and gene delivery. Adv Drug Deliv Rev 99(Part A):28–51. https://doi.org/10.1016/j.addr.2015.09.012
Takayama R, Ishizawa M, Yamada M, Inoue Y, Kanamoto I (2021) Characterization of Soluplus/ASC-DP nanoparticles encapsulated with minoxidil for skin targeting. ChemEngineering 5(3):44. https://doi.org/10.3390/chemengineering5030044
Tanida S, Kurokawa T, Sato H, Kadota K, Tozuka Y (2016) Evaluation of the micellization mechanism of an amphipathic graft copolymer with enhanced solubility of ipriflavone. Chem Pharm Bull 64:68–72. https://doi.org/10.1248/cpb.c15-00655
Tsukahara H, Matsuyama A, Abe T, Kyo H, Ohta T, Suzuki N (2016) Effects of intake of astaxanthin contained drink on skin condition. Japanese J Complement Altern Med 13:57–62. https://doi.org/10.1625/jcam.13.57
Wang C, Armstrong DW, Chang CD (2008) Rapid baseline separation of enantiomers and a mesoform of all-trans-astaxanthin, 13-cis-astaxanthin, adonirubin, and adonixanthin in standards and commercial supplements. J Chromatogr A 1194(2):172–177. https://doi.org/10.1016/j.chroma.2008.04.063
Wang Y, Wu Y, Wang T, Qiu D (2021) Isolation and identification of 9-cis astaxanthin by HPLC, FT-IR, and NMR spectra. J Appl Spectrosc 88:97–107. https://doi.org/10.1007/s10812-021-01146-y
Yang H, Teng F, Wang P, Tian B, Lin X, Hu X, Zhang L, Zhang K, Zhang Y, Tang X (2014) Investigation of a nanosuspension stabilized by Soluplus® to improve bioavailability. Int J Pharm 477(1–2):88–95. https://doi.org/10.1016/j.ijpharm.2014.10.025
Zarneshan SN, Fakhri S, Farzaei MH, Khan H, Saso L (2020) Astaxanthin targets PI3K/Akt signaling pathway toward potential therapeutic applications. Food Chem Toxicol 145:111714. https://doi.org/10.1016/j.fct.2020.111714
Zeng YC, Li S, Liu C, Gong T, Sun X, Fu Y, Zhang ZR (2017) Soluplus micelles for improving the oral bioavailability of scopoletin and their hypouricemic effect in vivo. Acta Pharmacol Sin 38:424–433. https://doi.org/10.1038/aps.2016.126
Zhang K, Yu H, Luo Q, Yang S, Lin X, Zhang Y, Tian B, Tang X (2013) Increased dissolution and oral absorption of itraconazole/Soluplus extrudate compared with itraconazole nanosuspension. Eur J Pharm Biopharm 85(3):1285–1292. https://doi.org/10.1016/j.ejpb.2013.03.002
Zhang L, Li Y, Yu JC (2014) Chemical modification of inorganic nanostructures for targeted and controlled drug delivery in cancer treatment. J Mater Chem B 2:452–470. https://doi.org/10.1039/c3tb21196g
Zheng YF, Bae SH, Kwon MJ, Park JB, Choi HD, Shin WG, Bae SK (2013) Inhibitory effects of astaxanthin, β-cryptoxanthin, canthaxanthin, lutein, and zeaxanthin on cytochrome P450 enzyme activities. Food Chem Toxicol 59:78–85. https://doi.org/10.1016/j.fct.2013.04.053
Zhu J, Zhuang P, Luan L, Sun Q, Cao F (2015) Preparation and characterization of novel nanocarriers containing krill oil for food application. J Funct Foods 19(Part B):902–912. https://doi.org/10.1016/j.jff.2015.06.017

## Publisher's Note